N. Jb. Miner. Abh. (J. Min. Geochem.) 197/3 (2022), 253–261
published online December 2, 2021, published in print January 2022

Article

Possibilities for misidentification of natural diamond and coesite in metamorphic rocks

Duncan S. Keller[1, 2, *], Jay J. Ague[1]

With 3 figures

Abstract: Coesite and diamond are the traditional indicator minerals used to identify ultrahigh-pressure (UHP) metamorphic rocks, which are rare records of deep subduction zone processes. However, concerns of UHP indicator misidentification and sample contamination drive dialogue on UHP discoveries. We document scenarios in which contamination artifacts or other mineral phases analytically or visually mimic genuine metamorphic diamond and coesite; these examples complement and extend discussion of sample contamination in suspected UHP rocks. Diamonds embedded or trapped during routine sample preparation can appear nearly identical to metamorphic diamond textures, including the radial polishing scratches that facilitate diamond recognition at thin section surfaces, and in some cases may not be dislodged by ultrasonic cleaning. The diagnostic Raman peak at or slightly above ~521 cm^{-1} used to identify coesite is close to Raman peaks of contaminant crystalline Si^0 from SiC grit (~521 cm^{-1}), and to photoluminescence excitations of rare earth elements in xenotime; these excitations may also mimic a coesite peak at ~424 cm^{-1}. To help avoid spurious recognition of diamond and coesite, we propose that surficial diamonds never be considered, that Si^0 and xenotime should be ruled out when proposing a coesite identification using Raman spectroscopy alone, and that inclusions < 5 µm from the slide base generally be excluded from consideration.

Keywords: microdiamond; coesite; contamination; ultrahigh-pressure metamorphism; indicator minerals

Introduction

Ultrahigh-pressure (UHP) metamorphic rocks are central to multidisciplinary study of subducting slabs and are unparalleled direct records of conditions in these environments (e.g., Sobolev & Shatsky 1990, Frezzotti et al. 2011, Gilotti 2013). Discoveries of UHP rocks have necessitated reconsideration of classic models for continental orogenesis (e.g., Chopin 1984, Smith 1984, Gilotti 2013) as well as locality-specific revisions of geologic histories. Traditionally, the polymorphic transition of quartz to coesite at ~2.5 to ~3 GPa (e.g., Mirwald & Massonne 1980) has been considered the lower bound of UHP conditions (Chopin 1984, Smith 1984); metamorphic microdiamonds signify UHP conditions > 3 GPa (Sobolev & Shatsky 1990, Frezzotti et al. 2011).

Although coesite and diamond can be readily identified using modern microanalytical techniques, the origins of these phases can be controversial. For example, the natural metamorphic growth of microdiamonds from some localities used to infer UHP subduction of continental crust has been questioned (e.g., Beyssac & Chopin 2003, Dobrzhinetskaya et al. 2014). Discovery of diamond, SiC, and Si^0 in mineral separates from ophiolites has led to debate over deep ophiolite formation and possible sample contamination (e.g., Robinson et al. 2004, Howell et al. 2015, Ballhaus et al. 2021). Additionally, hypotheses of metastable diamond formation at significantly lower pressures than ~3 GPa have prompted examination of mineral growth mechanisms and sample preparation practices (e.g., Farré-de-Pablo et al. 2019, Massonne 2019, Pujol-Solà et al. 2020).

Authors' addresses:

[1] Department of Earth and Planetary Sciences, Yale University, PO Box 208109, New Haven, CT 06520-8109 USA

[2] Department of Earth, Environmental and Planetary Sciences, Rice University, 6100 Main St., Houston, TX 77005 USA

* Corresponding author: dsk7@rice.edu

DOI: 10.1127/njma/2021/0313

www.schweizerbart.de
0077-7757/2021/0313 $ 2.25

On the geologic timescales of tectonic exhumation, coesite and diamond are expected to recrystallize to the lower-pressure polymorphs quartz and graphite unless included within minerals with high tensile strength such as garnet, pyroxene, or zircon that exert a strong confining pressure. In tectonically exhumed rocks, matrix coesite is very rarely observed (Liu et al. 2017) and matrix diamond is only known from the Kokchetav Massif (Schertl & Sobolev 2013). Recognition of these indicator minerals therefore usually relies on fully encapsulated grains identified with Raman spectroscopy or other nondestructive techniques operable below the surface of a thin section. Some studies also consider surficial inclusions. We present new documentation of contamination which mimics naturally-occurring diamond and coesite visually, analytically, or in both respects and suggest additional approaches to avoid misidentification.

Samples and Methods

The examples we present in this study are the result of routine thin section preparation of three rock types from the Brimfield Schist of the Central Maine Terrane in Connecticut, U.S.A. The first is a silica-undersaturated gneiss which records high-pressure granulite (HPG) facies conditions of ~1.8 GPa and ~1,040 °C ("the silica-undersaturated gneiss," Keller & Ague 2018). The second is a silica-saturated HPG gneiss (Ferrero et al. 2021) which also locally formed ultrahigh-temperature (UHT) assemblages ("the HPG/UHT gneiss;" Ague et al. 2013, Axler & Ague 2015). The third is another silica-saturated gneiss distinguished by exsolution lamellae of quartz, amphibole, mica, ilmenite, apatite, and rutile in garnet; the lamellae formed on the retrograde path following a UHP stage of $P \geq 5$ GPa ("the UHP gneiss;" Keller & Ague 2020). All of these rocks were exhumed as part of the same tectonic package and experienced UHT, granulite facies, and amphibolite facies overprints (Ague et al. 2013); minerals formed by these overprints developed to varying degrees in each rock type. Thin sections were prepared in the Yale University Department of Earth and Planetary Sciences. Billets were cut using a diamond-studded saw blade, then ground and polished using SiC grit down to 600 ANSI grit size (~15 µm diameter), followed by alumina to a grit size of 3 µm. Diamond polishing of thin and thick sections used diamond paste in successive grit sizes of 6, 3, 1, and 0.25 µm. Backscattered electron observation and cathodoluminescence (CL) excitation of diamonds were performed with the JEOL JXA-8530F field emission gun electron probe microanalyzer in the Yale University Department of Earth and Planetary Sciences. Raman spectroscopy followed the methods of Keller and Ague (2020). Analytical conditions for collecting the Raman spectra of Fig. 3a and 3d are 50× and 20× objective lenses, respectively, no filter, 532 nm laser wavelength, 400 µm hole, 150 µm slit, 1800 lines/mm grating, and 8 repetitions of 10 second analyses. Spectra were processed using CrystalSleuth (Lafuente et al. 2015) to remove backgrounds and cosmic ray interactions. Mineral abbreviations follow Whitney and Evans (2010).

Results

Diamond

During thin section preparation, small contaminant diamonds may be introduced into a sample and be mistaken for metamorphic microdiamond. Diamond-studded sawblades are ubiquitous in rock preparation and diamond abrasives are popular for the high-level polish the pastes impart, with grit sizes commonly ranging from 6 µm to 0.25 µm. Diamond-studded lapidary wheels may also implant diamond fragments during billet grinding; these diamonds could persist at depth in the final thin section, near the glass slide.

Microdiamonds protruding from garnet may readily be identified by the presence of radial polishing scratches surrounding the inclusion (e.g., Massonne et al. 1998, Kotková et al. 2011, Fig. 1a). In a study of >600 petrographic thin sections, Massonne et al. (1998) noted these scratches in UHP samples but extremely rarely (<1%) in lower-grade rocks. Embedding of contaminant diamond into phyllosilicates (Massonne et al. 1998) and zircon (Dobrzhinetskaya et al. 2014) is known, but implantation into garnet has seen little study. Despite testing of visual and/or spectroscopic methods for assessing whether or not a microdiamond is contaminant (Massonne et al. 1998, Beyssac & Chopin 2003, Perraki et al. 2009, Dobrzhinetskaya et al. 2014, Nasdala et al. 2016), a definitive test for genuine metamorphic diamonds remains elusive. The perfect octahedral cleavage of diamond allows polishing fragments to mimic the growth faces of a natural diamond.

After routine diamond polishing of a thin section of the silica-undersaturated gneiss, we observed seven diamonds ~3–7 µm in diameter protruding from a partially chloritized garnet, each displaying the distinctive radial scratch pattern (e.g. Fig. 1b). The diamonds were located only in trails of breached, empty fluid inclusions similar to those hosting naturally-occurring metamorphic diamonds (e.g., Sobolev & Shatsky 1990, Frezzotti et al. 2011). Cleaning of the sample in an ultrasonic bath at high power for three minutes dislodged six of the diamonds, but the seventh was so deeply embedded that it could not be removed regardless of the cleaning protocol. We noted no diamonds beneath the surface of the thin section, either petrographically or with Raman spectroscopy, and found no diamonds in a sample polished exclusively with alumina grit. There are no other mineralogical indicators of a UHP stage.

We also observed microdiamonds in breached fluid or melt inclusions at the surface of thin sections of the HPG/UHT gneiss polished with diamond paste (Fig. 1c–f). The

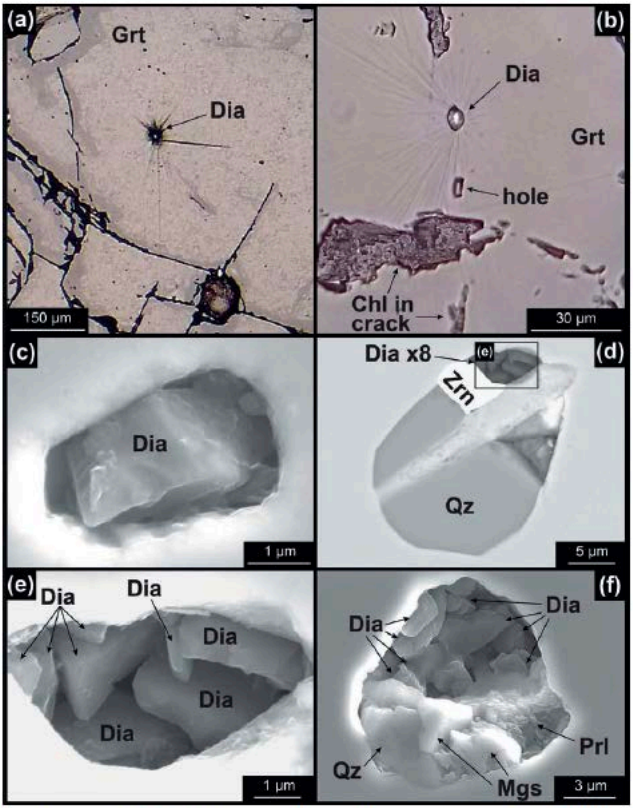

Fig. 1. Microdiamonds in garnet. (a) Reflected light image of a large naturally-occurring diamond from the UHP Saxonian Erzgebirge showing classic radial scratch pattern (Massonne et al. 1998). (b) Reflected light image of contaminant diamond embedded in garnet of the silica-undersaturated gneiss also showing radial scratches. (c–f) Backscattered electron images of contaminant diamonds in garnet from the UHT/HPG gneiss showing pervasive infill of breached inclusion void space. Mineral abbreviations follow Whitney and Evans (2010).

diamonds can have well-defined crystal faces (Fig. 1c), may occupy inclusions with other minerals (Fig. 1d, f), and may be plentiful within a given thin section. We excited the diamonds using CL and observed a range of fluorescence colors, including blue, yellow, pink, and green, often within the same thin section, and in some cases within the same inclusion. As in the silica-undersaturated gneiss, we did not find microdiamonds completely encased within garnet or in samples polished with alumina, and the diamonds are within the size range of the diamond pastes used in preparation. Preservation of metamorphic diamond is extremely unlikely because of the UHT, granulite facies, and amphibolite facies overprints that affected the HPG/UHT gneiss (Ague et al. 2013).

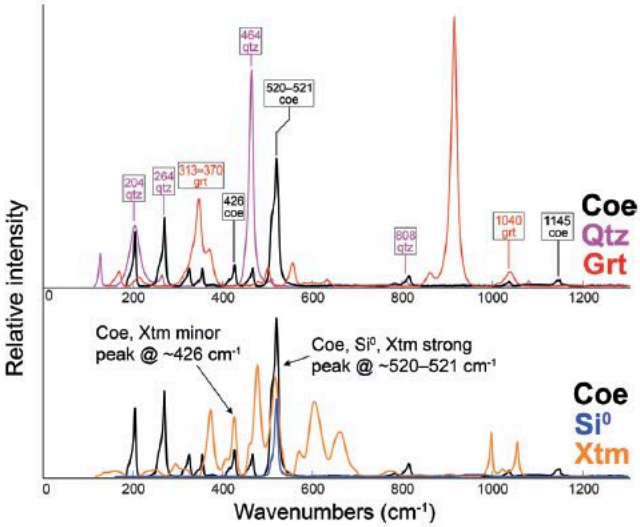

Fig. 2. Overlapping features of the coesite Raman spectrum with spectra of quartz, almandine, Si^0, and xenotime. The only coesite peaks that do not overlap with quartz or almandine are at 426 cm^{-1}, 520–521 cm^{-1}, and 1145 cm^{-1}. Labeled quartz and almandine peaks overlap with coesite peaks; labeled coesite peaks do not have overlaps. Coesite, Si^0, and xenotime all have a prominent peak at ~520–521 cm^{-1}. The coesite spectrum used is of a freestanding crystal with a peak at 520 cm^{-1}; coesite included in garnet and zircon from UHP terranes worldwide may show a peak at 521–526 cm^{-1} instead (e.g. Parkinson & Katayama 1999). Photoluminescence of REE in xenotime produces a peak at ~426 cm^{-1} (Lenz et al. 2015) that overlaps with a coesite peak. Spectra are from the RRUFF database (R070565, R040031, R060099, R050145, R050178; Lafuente et al. 2015). The y-axis has dimensionless units of relative intensity.

Coesite

Coesite misidentification has not been documented because coesite is not used in geological sample preparation. Coarse preserved coesite grains are commonly partially retrogressed and display a diagnostic "palisade texture" of coesite rimmed by polygranular quartz, typically surrounded by abundant radial cracks (e.g., Chopin 1984, Smith 1984). This distinctive texture allows partially retrogressed coesite to be identified visually. Small coesite grains fully enclosed in a strong host mineral such as garnet may be preserved; in these cases, Raman spectroscopy can be used to identify coesite beneath the surface of the host (e.g., Sobolev et al. 2000, Taguchi et al. 2021). However, coesite identification by Raman spectroscopy alone presents challenges, although this is rarely acknowledged. Each coesite peak except those at 426 cm^{-1}, 521 cm^{-1}, and 1145 cm^{-1} overlaps with quartz and/or almandine garnet peaks (Fig. 2). This means that only these three peaks could be assigned to coesite in a quartz-bearing inclusion in garnet without thorough spectral analysis (e.g., deconvolution, subtraction). It is important to note that each of these peaks may shift due to preserved strain or confining pressure. The strongest coesite peak, which at ambient conditions is at 520–521 cm^{-1}, may shift upward under residual pressure, reaching 532 cm^{-1} for coesite inclusions in diamond (Sobolev et al. 2000). Peaks as high as ~525–526 cm^{-1} are not uncommon for unfractured coesite in garnet or zircon (Parkinson & Katayama 1999). The coesite peak at ~1145 cm^{-1} may also shift closer to ~1160 cm^{-1} and overlap with a minor quartz peak (Osborne et al. 2019).

Importantly, peaks at ~521 cm^{-1} and ~426 cm^{-1} are not unique to coesite. The dominant coesite peak at 521 cm^{-1} overlaps with the strong peak of crystalline Si (Si^0) and a

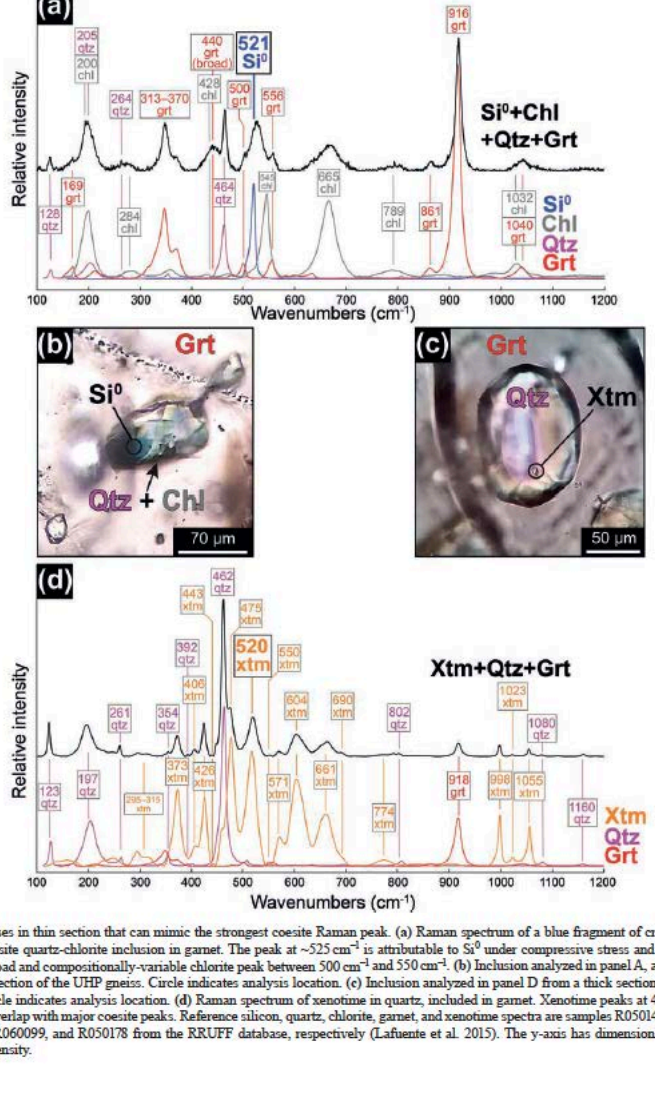

Fig. 3. Phases in thin section that can mimic the strongest coesite Raman peak. **(a)** Raman spectrum of a blue fragment of crystalline Si^0 in a composite quartz-chlorite inclusion in garnet. The peak at ~525 cm^{-1} is attributable to Si^0 under compressive stress and interactions with the broad and compositionally-variable chlorite peak between 500 cm^{-1} and 550 cm^{-1}. **(b)** Inclusion analyzed in panel A, at the bottom of a thick section of the UHP gneiss. Circle indicates analysis location. **(c)** Inclusion analyzed in panel D from a thick section of the UHP gneiss. Circle indicates analysis location. **(d)** Raman spectrum of xenotime in quartz, included in garnet. Xenotime peaks at 426 cm^{-1} and 520 cm^{-1} overlap with major coesite peaks. Reference silicon, quartz, chlorite, garnet, and xenotime spectra are samples R050145, R040031, R060188, R060099, and R050178 from the RRUFF database, respectively (Lafuente et al. 2015). The y-axis has dimensionless units of relative intensity.

photoluminescence excitation of Er^{3+} and possibly Tm^{3+} in xenotime (YPO_4; Lenz et al. 2015) (Fig. 2). Xenotime is a common accessory mineral, especially in metapelites. Si^0 can be a relict reactant of the industrial production of SiC grit (Greenwood and Earnshaw 1998, Ballhaus et al. 2021) and its strong peak at 521 cm^{-1} can mimic the asymmetry of the dominant coesite peak (Fig. 2). The minor coesite peak at ~426 cm^{-1} overlaps with peaks caused by photoluminescence of rare earth elements (REE) in xenotime (Fig. 2; Lenz et al. 2015) and a broad chlorite peak (Fig. 3a), hindering its use as a unique coesite identifier.

Further complications are posed by the common identification of coesite as fully encapsulated inclusions. Depending on the depth of the inclusion, the orientations of anisotropic minerals, the thicknesses of included phases, and the quality of the spectrum, the strength of Raman peaks can vary. Peaks of included phases may also shift due to anisotropic stresses (e.g., Bonazzi et al. 2019) created during decompression of inclusion and garnet host; wavenumber shifts can exceed 20 cm^{-1}. This increases the chances of relevant peak overlap with other phases. The limited range of diagnostic coesite peaks for a quartz-bearing inclusion in garnet, non-unique diagnostic peaks, and likely suppression of minor peaks together present considerable hindrances for identifying coesite in garnet by Raman spectroscopy alone, especially inclusions encased fully by garnet.

We report two examples of composite, quartz-bearing inclusions in garnet which show a prominent Raman peak overlapping with or near 521 cm^{-1} but which cannot be confirmed to contain coesite. The first example is a blueish-green grain in a quartz-chlorite inclusion at the bottom of a thick section of the UHP gneiss (Fig. 3b). The Raman peaks of quartz, chlorite, and a phase with a strong peak at ~525 cm^{-1} are somewhat suppressed relative to the garnet peaks because the section is ~150 μm thick. Multiple measurements of the grain yielded peaks in the range of 523–526 cm^{-1}; the spectrum in Figure 3 is typical. There are several problems with interpreting the blue-green inclusion in Figure 3b as coesite. First, there are no known examples of blue coesite, but coarse fragments of crystalline Si^0, which may be present as polishing contaminant, can be blue (Greenwood & Earnshaw 1998). Fine-grained Si^0 (e.g., < ~5 μm) is visually colorless. Second, the strongest coesite Raman peak at ~521 cm^{-1} is shared with Si^0 (Fig. 2). Third, no peak was noted at ~1145–1160 cm^{-1}. Finally, a chlorite peak at ~428 cm^{-1} hinders clear recognition of a coesite peak at ~426 cm^{-1} (Fig. 3a). Peaks of garnet, quartz, chlorite, and Si^0 are sufficient to reproduce the observed spectrum without the presence of coesite. Preserved compressive stress due to wedging of a Si^0 shard into garnet during polishing could positively shift the wavenumber of the ~521 cm^{-1} Si^0 peak by several cm^{-1} (e.g., Poborchii et al. 2006); additionally, convolution with the compositionally-variable and broad chlorite peak between ~500 cm^{-1} and 550 cm^{-1} may produce a composite peak shifted to slightly higher wavenumber. This effect appears poorly resolved due to the depth of the inclusion. We emphasize that unstressed contaminant Si^0 would show a Raman peak directly overlapping with the 521 cm^{-1} peak of unstressed coesite (e.g. Fig. 2).

In another thin section of the UHP gneiss, we analyzed a small grain (~10 μm) within a quartz inclusion exposed at the surface of its host garnet (Fig. 3c). The quartz inclusion shows a large anisotropic extinction halo in the surrounding garnet, suggesting preserved strain. We noted strong peaks at 520 cm^{-1} and 426 cm^{-1} that could be assigned to coesite. However, the additional presence of peaks at 373, 406, 475, 604, 661, 998, 1023, and 1055 cm^{-1} indicate that the mineral is xenotime (Fig. 3d).

Discussion

The examples we present offer opportunities to assess the ways in which genuine metamorphic diamond and coesite may be recognized in thin section. In the case of diamond, contamination by polishing material must be considered. In the case of coesite, both natural xenotime and contaminant Si^0 from SiC polishing grit should be ruled out when interpreting Raman spectroscopy results.

The diamonds we observed at thin section surfaces, although visually similar to genuine metamorphic diamond (Fig. 1), are within the size range of polishing grit. Their presence within breached inclusions, reminiscent of natural modes of diamond occurrence, is an expected outcome of polishing grit retention. Varied fluorescence characteristics suggest that the diamonds are a random sampling from different natural occurrences such as kimberlites, as would be expected for polishing material. Based on these traits, we conclude that the observed diamonds are contamination and that diamond fragments may be embedded into garnet during polishing and produce the radial scratch pattern associated with metamorphic microdiamonds (Fig. 1b). Such diamonds may be difficult or impossible to dislodge via ultrasonic cleaning.

Interpretations of diamonds in metamorphic rocks have also been shaped by suggestion of metastable diamond formation at pressures below the equilibrium stability of diamond (e.g., Massonne 2014, Pujol-Solà et al. 2020, Li et al. 2020). The examples of diamond contamination we present here reinforce concerns about the validity of all diamonds present in inclusion space that was ever in contact with preparation surfaces of the sample

(e.g., Dobrzhinetskaya et al. 2014, Massonne 2019). Testing of the hypothesis that diamond may form metastably in geologic environments would be best simplified and clarified by restricting discussion to samples prepared entirely without the use of diamond abrasives.

The Raman spectra we present with prominent peaks at or near 521 cm^{-1}, commonly considered diagnostic of coesite, cannot be assigned to coesite in our samples. The spectra and properties of the inclusions are instead consistent with Si^0 and xenotime (Fig. 3). The Si^0 peak is shifted to slightly higher wavenumber, likely due to a combination of preserved strain from implantation into the garnet and interactions with chlorite peaks at higher wavenumber. We conclude that Si^0 and xenotime included at depth in garnet, especially in quartz-bearing inclusions, present a risk of being misidentified as coesite based on Raman spectroscopy alone. Si^0 presents a particularly insidious problem because of its presence in a common polishing compound (Ballhaus et al. 2021). In our example of Si^0 contamination, the blue color of the Si^0 inclusion is readily apparent because the contaminant grain is coarse (~30 µm diameter), but finer-grained Si grit contamination would likely appear colorless. In this case, Si^0 could be visually indistinguishable from coesite. Si^0 contamination near the top or bottom of a thin section could be mistaken for coesite in a composite inclusion based on the presence of a peak at or near 521 cm^{-1}, especially if minor peaks were dampened (Fig. 2). Similarly, if a composite xenotime-bearing inclusion is at depth in the garnet and minor xenotime Raman and photoluminescence peaks are dampened, it is possible that coesite could be inferred using peaks at ~521 cm^{-1} and ~424 cm^{-1}. Standard thin section billet grinding using 600 grit will leave pits and scratches of up to several µm depth which could trap abrasives in the surface to be glued to a petrographic slide. We therefore recommend that only inclusions at least 5 µm away from the bottom of a slide should be used for UHP phase investigation.

Conclusions

We show that contaminant diamond may mimic the textures of metamorphic microdiamond at the surface of a thin section. Combined with previous work demonstrating the difficulty of distinguishing contaminant from naturally-occurring diamond (Beyssac & Chopin 2003, Perraki et al. 2009, Dobrzhinetskaya et al. 2014, Nasdala et al. 2016), it is clear that diamonds found near the upper or lower surfaces of a thin section are unsuitable for identifying UHP rocks. We urge that surficial microdiamonds of any kind, including those located near any surfaces of a thin section ever exposed to polishing materials, should not be considered as evidence of UHP conditions. Samples intended to showcase metamorphic microdiamonds should be polished completely without any diamond-bearing materials (e.g., with alumina), and if possible, should be prepared without diamond saws. We recommend that inclusions in garnet or other phases selected for study should be at least 5 µm above the glass slide for standard thin sections billets prepared with 600 SiC grit.

The strong Raman peak of coesite at ~521 cm^{-1} is commonly taken as a diagnostic identifier, but is non-unique and can be produced by polishing contamination artifacts. Peak overlaps from xenotime, quartz, and almandine-rich garnet further mask the unique properties of a coesite Raman spectrum in a composite inclusion in garnet. If a suspected coesite inclusion is fully encapsulated and does not display the classic palisade texture, identification by Raman spectroscopy alone can prove problematic depending on the orientation and depth of the inclusion and the location of analysis. Not all studies that identified coesite by Raman spectrum alone performed rigorous spectral decomposition to ensure the unambiguous presence of coesite. Misdiagnosis of coesite could result from undue weight given to the presence of a Raman peak at ~521–526 cm^{-1}, particularly for a composite inclusion at depth in garnet. Especially in cases where few analyses are presented, this could lead to spurious diagnosis of new UHP localities using only Raman data. We urge that coesite discoveries should be confirmed not to be Si^0 contamination or xenotime by thorough Raman spectroscopic characterization and spectral decomposition, chemical analyses by electron probe microanalysis (EPMA), and/or documentation of the diagnostic retrogressive palisade texture.

We raise these points not to call into question any specific study but to emphasize the pitfalls present when classifying a UHP rock based on diamond or coesite inclusions alone. We hope that by calling attention to possible contamination and misidentification scenarios, methods for identifying UHP rocks can be further refined. A UHP discovery can drastically change interpretations of an entire orogenic belt, so these rocks deserve particular scrutiny.

Acknowledgments: The authors acknowledge funding from Yale University and the US National Science Foundation Directorate of Geosciences (EAR-0744154, EAR-1250269, and EAR-1753553). We thank J.A. Axler, A.A. Haws, and E.M. Stewart for discussions, J. Girard for Raman technical support, J.O. Eckert Jr. for EPMA support, and K.K.M Lee for access to Raman facilities. We thank H.-J. Massonne for editorial handling and P. Liu for a constructive review. Comments from an anonymous reviewer on an earlier version improved this manuscript.

References

Ague, J. J., Eckert, J. O., Jr., Chu, X., Baxter, E. F., & Chamberlain, C. P. (2013). Discovery of ultrahigh-temperature metamorphism in the Acadian orogen, Connecticut, U.S.A. *Geology, 41*(2), 271–274. https://doi.org/10.1130/G33752.1

Axler, J. A., & Ague, J. J. (2015). Oriented multiphase needles in garnet from ultrahigh-temperature granulites, Connecticut, U.S.A. *The American Mineralogist, 100*(10), 2254–2271. https://doi.org/10.2138/am-2015-5018

Ballhaus, C., Helmy, H. M., Fonseca, R. O. C., Wirth, R., Schreiber, A., & Jöns, N. (2021). Ultra-reduced phases in ophiolites cannot come from Earth's mantle. *The American Mineralogist, 106*(7), 1053–1063. https://doi.org/10.2138/am-2021-7612

Beyssac, O., & Chopin, C. (2003). Comment on "Diamond, former coesite and supersilicic garnet in metasedimentary rocks from the Greek Rhodope: a new ultrahigh-pressure metamorphic province established" by E. D. Mposkos and D. K. Kostopoulos [*Earth and Planetary Science Letters, 192, 2001*] 497–506.

Bonazzi, M., Tumiati, S., Thomas, J. B., Angel, R. J., & Alvaro, M. (2019). Assessment of the reliability of elastic geobarometry with quartz inclusions. *Lithos, 350–351*, 105201. https://doi.org/10.1016/j.lithos.2019.105201

Chopin, C. (1984). Coesite and pure pyrope in high-grade blueschists of the Western Alps: A first record and some consequences. *Contributions to Mineralogy and Petrology, 86*(2), 107–118. https://doi.org/10.1007/BF00381838

Dobrzhinetskaya, L., Wirth, R., & Green, H. (2014). Diamonds in Earth's oldest zircons from Jack Hills conglomerate, Australia, are contamination. *Earth and Planetary Science Letters, 387*, 212–218. https://doi.org/10.1016/j.epsl.2013.11.023

Farré-de-Pablo, J., Proenza, J. A., González-Jiménez, J. M., Garcia-Casco, A., Colás, V., Roqué-Rossell, J., . . . Sánchez-Navas, A. (2019). A shallow origin for diamonds in ophiolitic chromitites. *Geology, 47*(1), 75–78. https://doi.org/10.1130/G45640.1

Ferrero, S., Ague, J. J., O'Brien, P. J., Wunder, B., Remusat, L., Ziemann, M. A., & Axler, J. (2021). High-pressure, halogen-bearing melt preserved in ultrahigh-temperature felsic granulites of the Central Maine Terrane, Connecticut (U.S.A.). *The American Mineralogist, 106*(8), 1225–1236. https://doi.org/10.2138/am-2021-7690

Frezzotti, M. L., Selverstone, J., Sharp, Z. D., & Compagnoni, R. (2011). Carbonate dissolution during subduction revealed by diamond-bearing rocks from the Alps. *Nature Geoscience, 4*(10), 703–706. https://doi.org/10.1038/ngeo1246

Gilotti, J. A. (2013). The realm of ultrahigh-pressure metamorphism. *Elements (Quebec), 9*(4), 255–260. https://doi.org/10.2113/gselements.9.4.255

Greenwood, N. N., & Earnshaw, A. (1998). *Chemistry of the Elements* (2nd ed.). Oxford: Butterworth-Heinemann.

Howell, D., Griffin, W. L., Yang, J., Gain, S., Stern, R. A., Huang, J.-X., . . . Pearson, N. J. (2015). Diamonds in ophiolites: Contamination or a new diamond growth environment? *Earth and Planetary Science Letters, 430*, 284–295. https://doi.org/10.1016/j.epsl.2015.08.023

Keller, D. S., & Ague, J. J. (2018). High-pressure granulite facies metamorphism (~1.8 GPa) revealed in silica-undersaturated garnet-spinel-corundum gneiss, Central Maine Terrane, Connecticut, U.S.A. *The American Mineralogist, 103*, 1851–1868.

Keller, D. S., & Ague, J. J. (2020). Quartz, mica, and amphibole exsolution from majoritic garnet reveals ultra-deep sediment subduction, Appalachian orogen. *Science Advances, 6*(11), eaay5178. https://doi.org/10.1126/sciadv.aay5178

Kotková, J., O'Brien, P. J., & Ziemann, M. A. (2011). Diamond and coesite discovered in Saxony-type granulite: Solution to the Variscan garnet peridotite enigma. *Geology, 39*(7), 667–670. https://doi.org/10.1130/G31971.1

Lafuente, B., Downs, R. T., Yang, H., & Stone, N. (2015). The power of databases: The RRUFF project. In T. Armbruster & R. M. Danisi (Eds.), *Highlights in Mineralogical Crystallography* (pp. 1–30). Berlin: Walter de Gruyter GmbH. https://doi.org/10.1515/9783110417104-003

Lenz, C., Nasdala, L., Talla, D., Hauzenberger, C., Seitz, R., & Kolitsch, U. (2015). Laser-induced REE^{3+} photoluminescence of selected accessory minerals – An "advantageous artefact" in Raman spectroscopy. *Chemical Geology, 415*, 1–16. https://doi.org/10.1016/j.chemgeo.2015.09.001

Li, B., Massonne, H.-J., Koller, F., & Zhang, J. (2020). Metapelite from the high-to ultrahigh-pressure terrane of the Eastern Alps (Pohorje Mountains, Slovenia) – New pressure, temperature and time constraints on a polymetamorphic rock. *Journal of Metamorphic Geology, 39*(6), 695–726. https://doi.org/10.1111/jmg.12581

Liu, P., Massonne, H.-J., Zhang, J., Wu, Y., & Jin, Z. (2017). Intergranular coesite and coesite inclusions in dolomite from the Dabie Shan: Constraints on the preservation of coesite in UHP rocks. *Terra Nova, 29*(3), 154–161. https://doi.org/10.1111/ter.12258

Massonne, H.-J. (2014). Wealth of P–T–t information in medium-high grade metapelites: Example from the Jubrique Unit of the Betic Cordillera, S Spain. *Lithos, 208–209*, 137–157. https://doi.org/10.1016/j.lithos.2014.08.027

Massonne, H.-J. (2019). Comment: A shallow origin for diamonds in ophiolitic chromitites. *Geology, 47*(8), e476. https://doi.org/10.1130/G46459C.1

Massonne, H.-J., Bernhardt, H.-J., Dettmar, D., Kessler, E., Medenbach, O., & Westphal, T. (1998). Simple identification and quantification of microdiamond in rock thin-sections. *European Journal of Mineralogy, 10*(3), 497–504. https://doi.org/10.1127/ejm/10/3/0497

Mirwald, P. W., & Massonne, H.-J. (1980). The low-high quartz and quartz-coesite transition to 40 kbar between 600 °C and 1600 °C and some reconnaissance data on the effect of $NaAlO_2$ component on the low quartz–coesite transition. *Journal of Geophysical Research, 85*(B12), 6983–6990. https://doi.org/10.1029/JB085iB12p06983

Nasdala, L., Steger, S., & Reissner, C. (2016). Raman study of diamond-based abrasives, and possible artefacts in detecting UHP microdiamond. *Lithos, 265*, 317–327. https://doi.org/10.1016/j.lithos.2016.03.009

Osborne, Z. R., Thomas, J. B., Nachlas, W. O., Baldwin, S. L., Holycross, M. E., Spear, F. S., & Watson, E. B. (2019). An experimentally calibrated thermobarometric solubility model for titanium in coesite (TitaniC). *Contributions to Mineralogy and Petrology, 174*(4), 34. https://doi.org/10.1007/s00410-019-1575-5

Parkinson, C. D., & Katayama, I. (1999). Present-day ultrahigh-pressure conditions of coesite inclusions in zircon and garnet: Evidence from laser Raman microspectroscopy. *Geology, 27*(11), 979–982. https://doi.org/10.1130/0091-7613(1999)0272.3.CO;2

Perraki, M., Korsakov, A. V., Smith, D. C., & Mposkos, E. (2009). Raman spectroscopic and microscopic criteria for the distinction of microdiamonds in ultrahigh-pressure metamorphic rocks from diamonds in sample preparation. *The American Mineralogist, 94*(4), 546–556. https://doi.org/10.2138/am.2009.2973

Poborchii, V., Tada, T., & Kanayama, T. (2006). High-spatial-resolution Raman microscopy of stress in shallow-trench-isolated Si

structures. *Applied Physics Letters, 89*(23), 233505. https://doi.org/10.1063/1.2400057

Pujol-Solà, N., Garcia-Casco, A., Proenza, J. A., González-Jiménez, J. M., del Campo, A., Colás, V., . . . Roqué-Rosell, J. (2020). Diamond forms during low pressure serpentinisation of oceanic lithosphere. *Geochemical Perspectives Letters, 15*, 19–24. https://doi.org/10.7185/geochemlet.2029

Robinson, P. T., Bai, W.-J., Malpas, J., Yang, J.-S., Zhou, M.-F., Fang, Q.-S., . . . Staudigel, H. (2004). Ultra-high pressure minerals in the Luobusa Ophiolite, Tibet, and their tectonic implications. *Special Publication – Geological Society of London, 226*(1), 247–271. https://doi.org/10.1144/GSL.SP.2004.226.01.14

Schertl, H.-P., & Sobolev, N. V. (2013). The Kokchetav Massif, Kazakhstan: "Type locality" of diamond-bearing UHP metamorphic rocks. *Journal of Asian Earth Sciences, 63*, 5–38. https://doi.org/10.1016/j.jseaes.2012.10.032

Smith, D. C. (1984). Coesite in clinopyroxene in the Caledonides and its implications for geodynamics. *Nature, 310*(5979), 641–644. https://doi.org/10.1038/310641a0

Sobolev, N. V., Fursenko, B. A., Goryainov, S. V., Shu, J., Hemley, R. J., Mao, H., & Boyd, F. R. (2000). Fossilized high pressure from the Earth's deep interior: The coesite-in-diamond barometer. *Proceedings of the National Academy of Sciences of the United States of America, 97*(22), 11875–11879. https://doi.org/10.1073/pnas.220408697

Sobolev, N. V., & Shatsky, V. S. (1990). Diamond inclusions in garnets from metamorphic rocks: A new environment for diamond formation. *Nature, 343*(6260), 742–746. https://doi.org/10.1038/343742a0

Taguchi, T., Kouketsu, Y., Igami, Y., Kobayashi, T., & Miyake, A. (2021). Hidden intact coesite in deeply subducted rocks. *Earth and Planetary Science Letters, 558*, 116763. https://doi.org/10.1016/j.epsl.2021.116763

Whitney, D. L., & Evans, B. W. (2010). Abbreviations for names of rock-forming minerals. *The American Mineralogist, 95*(1), 185–187. https://doi.org/10.2138/am.2010.3371

Manuscript received: October 2, 2021
Revisions requested: October 4, 2021
Revised version received: October 23, 2021
Accepted: October 26, 2021
Responsible editor: H.-J. Massonne